JOURNAL OF MOLECULAR SPECTROSCOPY 77, 402–428 (1979)

# Rotational Analysis of the $NO_2$ 6125-Å Region

D. L. MONTS,[1] B. SOEP,[2] AND R. N. ZARE[3]

*Department of Chemistry, Columbia University, New York, New York 10027*

In the $NO_2$ 6125-Å region 135 transitions belonging to four bands have been assigned using laser-induced fluorescence. On the whole, the rotational structure of the four vibronic bands is well characterized by near-prolate symmetric top relations. The 6125 and 6126-Å bands perturb each other, the former having predominantly the character of the $\tilde{A}^2B_2$ state, the latter the $\tilde{X}^2A_1$ state; this parent–daughter relationship is recognized to occur elsewhere in the $NO_2$ visible spectrum.

## I. INTRODUCTION

After approximately one man-millenium of work, an understanding of the $NO_2$ visible spectrum is emerging (*1*). In 1965 the analysis by Douglas and Huber (*2*) of $^2B_1K_a = 0$ levels established the importance of Renner–Teller interaction in the $NO_2$ visible spectrum. The following year Douglas (*3*) suggested that much of the complexity of the system might arise from vibronic coupling between an excited electronic state and high vibrational levels of the ground state. In the early 1970s rotational analyses of $NO_2$ transitions coincident with fixed-frequency laser lines (*4–6*) confirmed the existence of at least two electronic states in the visible, $^2B_1$ and $^2B_2$. Analysis of the 5933-Å band (*7–9*) firmly established the predominance of the $^2B_2$ state in the red region. Subsequent work (*10, 11*) has shown that extensive vibronic coupling between $\tilde{A}^2B_2$ and high vibrational levels of the $\tilde{X}^2A_1$ state does account for most of the vibronic bands in the visible. However, theoretical calculations (*12*) place the ground state barrier to linearity (the origin of $^2B_1$) at 13 400 $cm^{-1}$ and indicate the presence of a third excited electronic state, $^2A_2$, predicted to lie at 14 800 $cm^{-1}$ above the ground state. Inspection of low resolution $NO_2$ absorption spectra (*1*) shows a sudden and drastic increase in the complexity of the spectrum at wavelengths shorter than about 5700 Å; currently, it appears that at energies less than ~17 500 $cm^{-1}$ Franck–Condon factors may not be favorable for $^2B_1$–$^2A_1$ or $^2A_2$–$^2A_1$ transitions.

The present study was begun with the hope that the analysis of another $NO_2$ band by the method of laser-induced fluorescence would supplement the current level of understanding and might prove instrumental in recognizing in more detail what gives the $NO_2$ visible spectrum its complex appearance. The 6125-Å region is chosen because it is accessible with available tunable dye laser sources,

[1] Present address: Department of Chemistry, Rice University, Houston, Texas 77001.

[2] Present address: Laboratoire Photophysique Moleculaire, CNRS, Universite Paris-Sud, 91405 Orsay, France.

[3] Present address: Department of Chemistry, Stanford University, Stanford, California 94305.

0022-2852/79/100402-27$02.00/0



Copyright © 1979 by Academic Press, Inc.
All rights of reproduction in any form reserved.

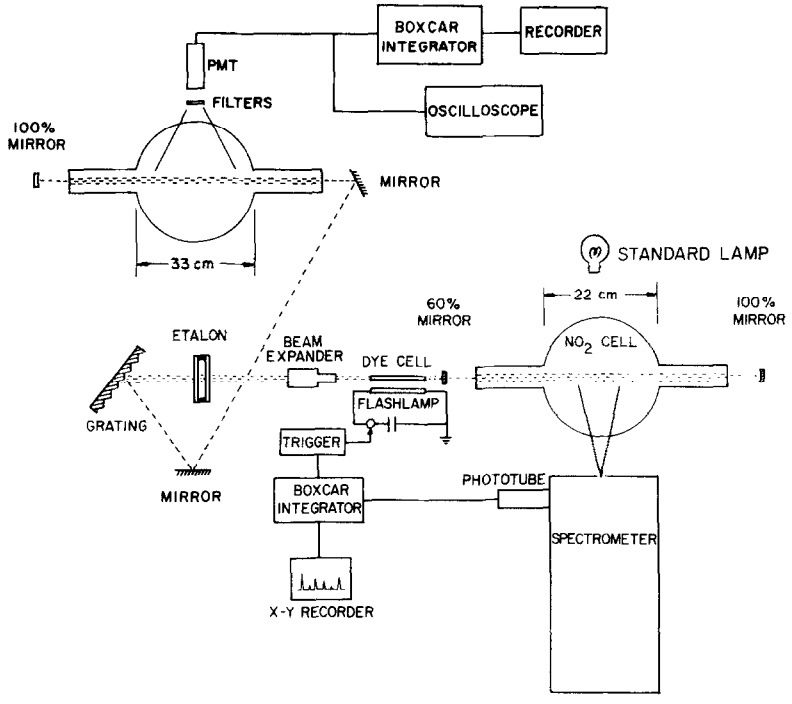


FIG. 1. Schematic diagram of the experimental apparatus.

and because this spectral region is expected to be comprised of $B_2$ vibronic bands and free of complexities introduced by the presence of $B_1$ or $A_2$ vibronic bands. Inspection of microdensitometer traces reveals that the appearance of the 6125-Å region is relatively simple, suggesting that the 6125-Å band is not severely overlapped and might be relatively unperturbed. Furthermore, there appears to be an abundance of strong, isolated transitions, making this region a logical choice for investigation.

## II. EXPERIMENTAL DETAILS

The experimental apparatus, shown in Fig. 1, is a modified version of that used by Stevens and Zare (*8*). The active medium of the dye laser consists of rhodamine 6G (R6G) dissolved in a 5% solution of the detergent Ammonyx LO in water; the dye laser concentration is adjusted to minimize the threshold for lasing. Typically the laser is operated at a pulse rate of 5 pps. The dye laser can maintain a chosen wavelength for ~45 min, during which time several fluorescence spectra can be recorded. Laser bandwidths of 0.05–0.13 $cm^{-1}$ were obtained by use of an 1800 line/mm diffraction grating (PTR Optics TR-R2 grating) operated in first order in conjunction with a 6× beam expander and a temperature-stabilized etalon (Coherent Radiation Model 760) with a 0.9-$cm^{-1}$ free spectral range. Excitation spectra could be produced by scanning through the free spectral range of the etalon; such an excitation spectrum is shown in Fig. 2. Here the

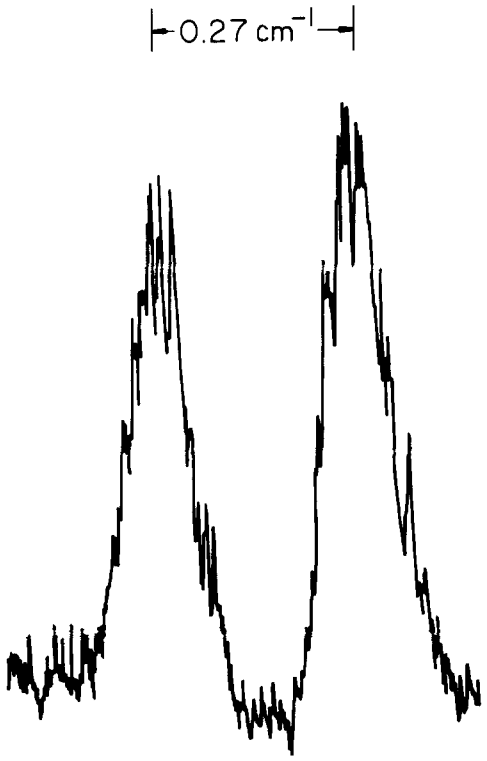


FIG. 2. Excitation spectrum of the 16 359.26- and 16 359.53-$cm^{-1}$ transitions; the latter transition is on the right. The observed FWHM is 0.078 $cm^{-1}$; the Doppler width (FWHM) of the transition is 0.03 $cm^{-1}$.

observed linewidth (0.078 $cm^{-1}$ FWHM) is a convolution of the laser bandwidth and the Doppler width of the line (0.03 $cm^{-1}$ FWHM). The excitation spectrum is a sum of 3000 laser shots and thus laser jitter, if random, is averaged out. For the purposes of this study, no advantage would have been obtained by further reducing the laser bandwidth.

The fluorescence is monitored at right angles to the excitation direction with a 1-m spectrometer (Spex 1704) operated in second order. The signal is detected by an extended S-20 phototube (EMI 9658 R) which was chosen for its high quantum efficiency in the red. Phototube output is fed through a cathode follower into a boxcar integrator (PAR Model CW-1) that accumulated signal during a 50-$\mu$sec window with a 4-$\mu$sec delay. With the use of an oscilloscope the boxcar is triggered off the radio frequency noise generated by the laser discharge. The spectrometer is mechanically scanned by a stepping motor (Spex stepper control Model 1751-5). Low resolution fluorescence spectra are recorded at 90 Å/min with 2-mm-wide slits. Rotationally-resolved fluorescence spectra are recorded at 1.8 or 3.6 Å/min with slit widths of 150 to 700 $\mu$m; using a standard scan setting on the X–Y recorder, the observed scan rates are 1.4 or 2.8 $cm^{-1}$/cm, respectively, for fluorescence to $2\nu_2''$. Wavelength markers are placed on the spectrum by man-

ually depressing a momentary contact switch that connects the recorder with a battery. For each rotationally resolved fluorescence spectrum, three or more pairs of wavelength markers are used to determine the scan rate (in Å/cm). A spectrum is rejected if the scan rates differ by more than ±0.02 Å/cm; this uncertainty includes error due to spectrometer wavelength drive nonlinearity, recorder nonlinearity, and human error. The scan rate appears to differ (up to ~2%) from scan to scan, but for a given scan the rate is constant. An absolute frequency calibration mark is recorded for each rotationally resolved spectrum by continuously scanning the spectrometer through the $NO_2$ fluorescence and through standard Ar lines obtained from an Osram Cd spectral lamp positioned as shown in Fig. 1. After the $NO_2$ fluorescence is recorded and while the spectrometer is still scanning, the spectrometer slit widths and the phototube voltage are reduced and the spectral lamp is started; the output of the phototube is fed into a picoammeter (Keithley Model 417) and then to an L & N recorder. As the spectrometer is observed to scan through the maximum of the standard line, a wavelength marker is recorded on the X–Y recorder spectrum. With this procedure we observe an uncertainty in the $NO_2$ fluorescence peak positions of ±0.1 Å.

The dye laser is tuned to the desired wavelength by use of the spectrometer. As the spectrometer scans at 0.9 Å/min through a standard atomic line, a timer (Standard Electric Time Co. Type 5-60) is started; after the passage of a time interval corresponding to the wavelength difference between a standard atomic line and the desired wavelength, both the timer and the spectrometer are stopped. The laser beam is deflected through a diffuser into the spectrometer. The laser is then tuned to the wavelength at which the spectrometer is set and the fluorescence maximized. The time interval required to mechanically scan the spectrometer between a standard atomic line and the laser is measured before and after each rotational spectrum. A temporal uncertainty of ±1 sec results in a wavelength uncertainty of ±0.015 Å. The scan speed of the spectrometer has been calibrated on two occasions by measuring the spectrometer scan time between standard atomic lines. The observed scan rates are 0.87 ± 0.02 Å/min (four measurements) and 0.90 ± 0.01 Å/min (seven measurements); the quoted uncertainties are the 90% confidence limits. The other spectrometer scan speeds used display similar errors. Standard atomic lines from Osram spectral lamps of Ne, Cd, and Hg and from a Th electrodeless discharge lamp are used in the laser-tuning procedure.

Lifetimes of selected, unblended $NO_2$ transitions are measured simultaneously with the fluorescence spectrum. This is achieved by reflecting the laser light diffracted in zeroth order by the grating through a separate 33-cm diameter fluorescence cell. The fluorescence is detected by an extended S-20 phototube (Centronic Q4283 SA-25). By placing Corning 2-60 and 2-59 filters between the phototube and the cell, the laser radiation is attenuated by a factor of $\sim 10^4$. Fluorescence decay curves can be recorded by either photographing the fluorescence decay excited by a single laser pulse or by scanning with a boxcar integrator. Lifetimes are obtained with the boxcar using a 200-$\mu$sec time base duration, a 5-$\mu$sec rate, and a 10-min scan time; three scans are taken for each transition so measured and the decrease in laser intensity as a function of time compensated.

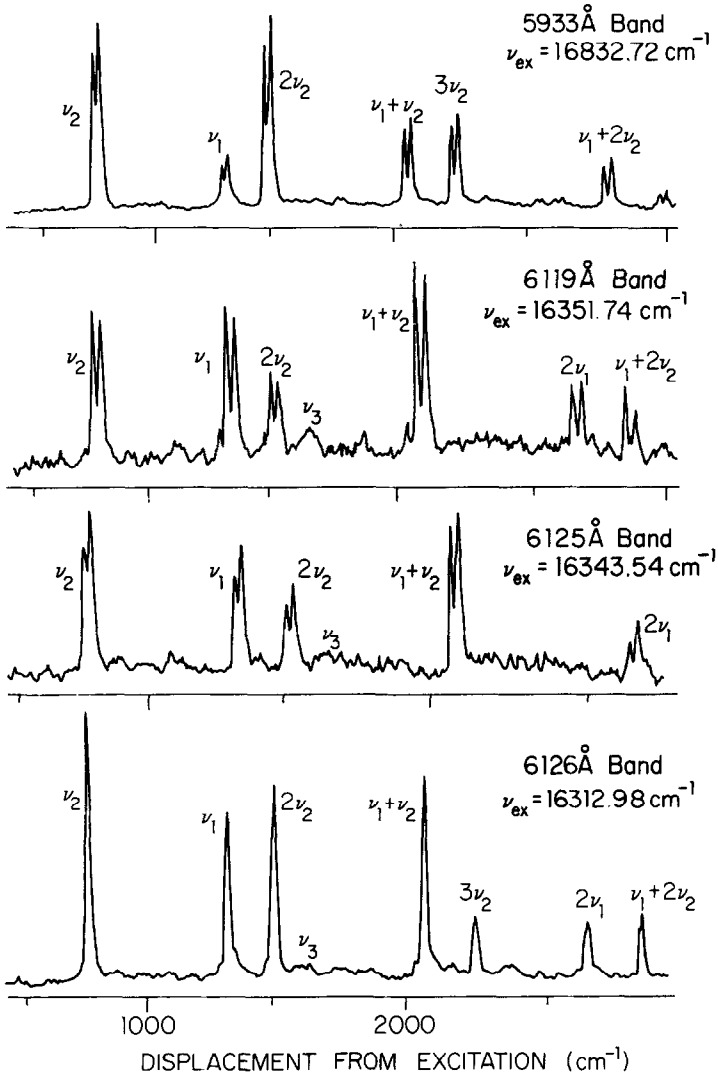


FIG. 3. Low resolution fluorescence spectra. The $NO_2$ pressure is typically 50 mTorr. These spectra were obtained using the amplitude-stabilized (±3%) cw dye laser described by Figger *et al.* (*29*).

Three photographs are taken of each fluorescence decay showing the initial 90 or 180 μsec of decay; the three lifetimes obtained are averaged. Within experimental error, lifetimes obtained from photographs and from boxcar averaging are identical.

Lifetime measurements are made at pressures of ≤1 mTorr as measured by a capacitance manometer (Datametrics Type 1023 with Type 523-15 pressure sensor). Fluorescence spectra are taken using $NO_2$ pressures of typically 50 mTorr as measured by a thermocouple gauge (Veeco Model TG-7 with type DVLM gauge tube).

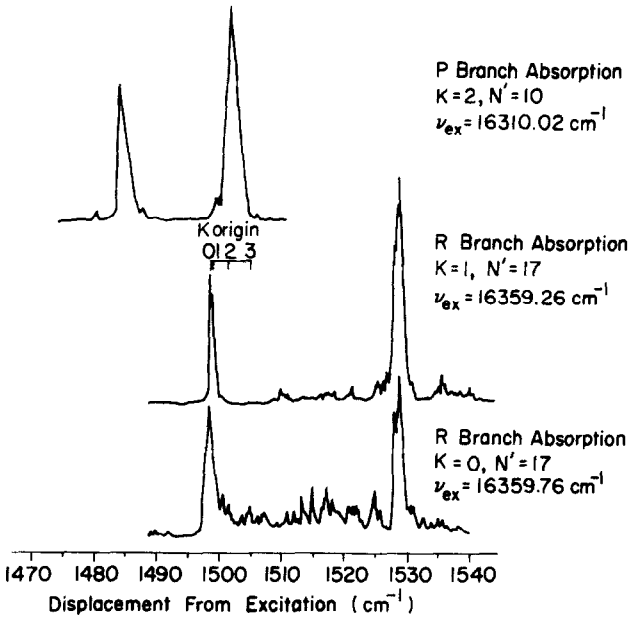


FIG. 4. Rotationally resolved $NO_2$ fluorescence to $2\nu_2''$.

A purified $NO_2$ sample is stored in a liquid-nitrogen-cooled coldfinger. Contaminants are eliminated from the sample by removing the liquid nitrogen bath and pumping away the contaminants, which are themselves more volatile than $NO_2$ at these temperatures. We note that after a few hours of laser irradiation, unassigned peaks appear in the vibrational fluorescence spectrum at positions where no vibrational fluorescence is expected; this phenomenon does not affect the rotational analysis, but frequent change of sample is advisable to avoid a potentially complicating factor in lifetime studies.

The high resolution absorption spectrum was photographed in second order using the Argonne National Laboratory 9.15-m concave-grating spectrograph (*1*). Line positions were measured relative to Th emission line standards using a Grant comparator located in the Columbia University Chemistry Department. The reproducibility of unblended lines is $\pm 0.004$ cm$^{-1}$. Using plates photographed by Douglas and Huber (*2*), Lee has measured the $NO_2$ line positions in the 6125-Å region. Peck (*13*) has provided us with a listing of Lee's line positions, which agree with our positions to within $\pm 0.010$ cm$^{-1}$. The 6125-Å region has also been measured by Hsu (*1*); in this case, the agreement between the line position measurements reported here and those of Hsu is within $\pm 0.004$ cm$^{-1}$.

## III. RESULTS

### *A. Line Position Assignments*

Analysis of the 6125-Å region indicates that there are four vibronic bands of significant intensity in the 6110- to 6130-Å region: 6117, 6119, 6125, and 6126 Å. Figure 3 shows low resolution spectra, uncorrected for photomultiplier and spec-

TABLE I

Rotational Assignments in the 6125-Å Region in the $NO_2$ $^2B_2 \leftarrow {}^2A_1$ Transition

| $N'_{K_a,K_c}$ | $N''_{K_a,K_c}$ | $\nu$ (cm$^{-1}$) | $N''_{K_a,K_c}$ | $\nu$ (cm$^{-1}$) | obs − calc (cm$^{-1}$) $F_1$ | $F_2$ |
|---|---|---|---|---|---|---|
| | | The 6117Å Band | | | | |
| $1_{01}$ | $0_{00}$ | 16 343.28[a] | $2_{02}$ | 16 340.78[a] | -0.03 | -0.03 |
| | | 344.08[a] | | | | |
| $3_{03}$ | $2_{02}$ | 344.87[a] | $4_{04}$ | 338.98[a] | -0.02 | -0.02 |
| | | 345.32[a] | | 339.39[a] | 0.02 | 0.02 |
| $5_{05}$ | $4_{04}$ | 346.28[a] | $6_{06}$ | 337.03[a] | -0.03 | -0.03 |
| | | 346.49[a] | | 337.24[a] | -0.03 | -0.03 |
| $17_{0,17}$ | $16_{0,16}$ | 359.76[b] | $18_{0,18}$ | 330.36[c] | -0.03 | -0.03 |
| $19_{0,19}$ | $18_{0,18}$ | 361.69[b] | $20_{0,20}$ | 328.91[b] | 0.01 | 0.01 |
| $13_{1,12}$ | $12_{1,11}$ | 353.35[b] | $14_{1,13}$ | 330.21[c] | 0.05 | 0.05 |
| $15_{1,14}$ | $14_{1,13}$ | 356.45[b] | $16_{1,15}$ | 329.94[b] | 0.01 | 0.01 |
| $17_{1,16}$ | $16_{1,15}$ | 359.26[b] | $18_{1,17}$ | 329.29(41)[d] | 0.06 | -0.06 |
| | | 359.53[b] | | 329.61[c] | 0.01 | 0.01 |
| | | The 6119Å Band | | | | |
| $1_{01}$ | $0_{00}$ | 16 337.80[a] | $2_{02}$ | 16 335.27[a] | 0.00 | 0.00 |
| $11_{1,10}$ | $10_{1,9}$ | 346.04[b] | $12_{1,11}$ | 326.38[c] | -0.01 | -0.01 |
| $13_{1,12}$ | $12_{1,11}$ | 347.10[b] | $14_{1,13}$ | 324.02[c] | -0.01 | -0.01 |
| $15_{1,14}$ | $14_{1,13}$ | 348.15[b] | $16_{1,15}$ | 321.65[c] | 0.00 | 0.00 |
| $21_{1,20}$ | $20_{1,19}$ | 351.74[b] | $22_{1,21}$ | 315.04[b] | -0.02 | -0.02 |
| | | The 6125Å Band | | | | |
| $1_{01}$ | $0_{00}$ | 16 321.79[a] | $2_{02}$ | 16 319.25[a] | 0.01 | 0.01 |
| | | 322.71[a] | | 320.13[a] | 0.05 | 0.05 |
| $3_{03}$ | $2_{02}$ | 324.02[a,b] | $4_{04}$ | 318.11[a,c] | 0.00 | 0.00 |
| | | 324.50[a] | | 318.55[a] | 0.04 | 0.04 |
| $5_{05}$ | $4_{04}$ | 325.99[a] | $6_{06}$ | 316.69[a] | 0.02 | 0.02 |
| | | 326.38[a] | | 317.12[a] | -0.02 | -0.02 |
| $1_{10}$ | $1_{11}$ | 325.72[b] | $2_{11}$ | 323.92[b] | | 0.02 |
| $2_{12}$ | $1_{11}$ | 327.62[c,e] | $3_{13}$ | 323.38[b,e] | | 0.01 |
| | | 328.12[b,e] | | 323.98[b,e] | 0.01 | |
| $3_{12}$ | $2_{11}$ | 328.43[c,e] | $4_{13}$ | 322.40[b,e] | | 0.02 |
| | | 329.14[b,e] | | 323.18[b,e] | -0.02 | |
| $5_{14}$ | $4_{13}$ | 331.17[b,e] | $6_{15}$ | 321.79[b,e] | -0.03 | |
| $7_{16}$ | $6_{15}$ | 331.02[b] | $8_{17}$ | 318.16[c] | | 0.02 |
| | | 333.27[b,e] | | 320.41[b,e] | 0.03 | |
| $10_{1,10}$ | $9_{19}$ | 335.05[b] | $11_{1,11}$ | 317.57[c] | 0.01 | 0.00 |
| $12_{1,12}$ | $11_{1,11}$ | 336.79[b] | $13_{1,13}$ | 315.99[c] | 0.00 | 0.00 |
| | | 337.03[b] | | 316.22[c] | 0.01 | 0.01 |
| $13_{1,12}$ | $12_{1,11}$ | 338.19[b] | $14_{1,13}$ | 315.10[b] | 0.00 | 0.00 |
| $16_{1,16}$ | $15_{1,15}$ | 340.78[b] | $17_{1,17}$ | 313.35[c] | -0.01 | -0.01 |
| $18_{1,18}$ | $17_{1,17}$ | 340.82[b] | $19_{1,19}$ | 310.08[b] | -0.02 | -0.02 |
| | | 343.54[b] | | 312.76[c] | 0.02 | 0.02 |

trometer response. A fluorescence spectrum from a member of the 6117-Å band is not shown, but the intensity distribution appears to be similar to that of the 6126-Å band. The double peaks observed in the 5933, 6119, and 6125-Å spectra are *R* and *P* branch transitions, which are resolved even at this resolution because the ground state energy separations of the transitions excited are relatively large.

The Franck–Condon factors in the 6125-Å region differ significantly from those in the 5933-Å region; in particular, fluorescence to $\nu_1''$ and $2\nu_1''$ is more pronounced

TABLE I—*Continued*

| $N'_{K_a,K_c}$ | $N''_{K_a,K_c}$ | $\nu$ (cm$^{-1}$) | $N''_{K_a,K_c}$ | $\nu$ (cm$^{-1}$) | obs - calc (cm$^{-1}$) $F_1$ | $F_2$ |
|---|---|---|---|---|---|---|
| $22_{1,22}$ | $21_{1,21}$ | 16 349.12[c] | $23_{1,23}$ | 16 311.72[b] | 0.01 | 0.01 |
| $2_{21}$ | $2_{20}$ | 322.71[b,e] | $3_{22}$ | 320.13[c,e] | | -0.01 |
| | | 324.17[c,e] | | 321.65[b,e] | 0.02 | |
| $5_{23}$ | $4_{22}$ | 327.98[b,e] | $6_{24}$ | 318.68[c,e] | | -0.02 |
| $6_{25}$ | $5_{24}$ | 329.01[b,e] | $7_{26}$ | 318.02[c,e] | | -0.01 |
| $8_{27}$ | $7_{26}$ | 331.14[b,e] | $9_{28}$ | 316.77[c,e] | | 0.01 |
| $9_{27}$ | $8_{26}$ | 331.58[c] | $10_{28}$ | 315.56[b] | -0.02 | |
| $11_{29}$ | $10_{28}$ | 335.27[b,e] | $12_{2,10}$ | 315.84[c,e] | 0.00 | |
| $12_{2,11}$ | $11_{2,10}$ | 335.76[b,e] | $13_{2,12}$ | 314.65[c,e] | | 0.01 |
| | | 336.16[b,e] | | 315.04[b,e] | 0.03 | |
| $13_{2,11}$ | $12_{2,10}$ | 337.08[b] | $14_{2,12}$ | 314.24[c] | 0.02 | 0.01 |
| | | The 6126Å Band | | | | |
| $1_{01}$ | $0_{00}$ | 16 319.93[a,f] | $2_{02}$ | 16 317.41[a,f] | -0.01 | -0.01 |
| $3_{03}$ | $2_{02}$ | 321.31[a,b,f] | $4_{04}$ | 315.41[a,b,f] | -0.01 | -0.01 |
| $5_{04}$ | $4_{04}$ | 322.25[a,b,f] | $6_{06}$ | 312.98[a,b,f] | -0.01 | -0.01 |
| $7_{07}$ | $6_{06}$ | 323.83[b,f] | $8_{08}$ | 311.18[b,f] | 0.00 | 0.00 |
| $9_{09}$ | $8_{08}$ | 324.86[c,f] | $10_{0,10}$ | 308.82[b,f] | 0.02 | 0.02 |
| $5_{14}$ | $4_{13}$ | 323.66[b,f] | $6_{15}$ | 314.24[c,f] | 0.01 | 0.00 |
| $7_{16}$ | $6_{15}$ | 324.98[c,f] | $8_{17}$ | 312.15[b,f] | 0.00 | -0.01 |
| $8_{18}$ | $7_{17}$ | 325.07[c] | $9_{19}$ | 310.94[b] | -0.01 | -0.02 |
| | | 325.26[b] | | 311.13[b] | -0.01 | -0.02 |
| $9_{18}$ | $8_{19}$ | 326.27[b,f] | $10_{19}$ | 310.02[b,f] | 0.00 | -0.01 |
| $3_{21}$ | $2_{20}$ | 323.26[b,f] | $4_{22}$ | 317.24(.41)[d] | -0.01 | 0.02 |
| | | 323.98[b] | | 317.97(8.11)[d] | 0.01 | 0.01 |
| $5_{23}$ | $4_{22}$ | 324.86[b] | $6_{24}$ | 315.56[c] | 0.03 | -0.02 |
| $6_{25}$ | $5_{24}$ | 325.26[b,f] | $7_{26}$ | 314.24(.29)[d] | 0.01 | 0.02 |
| $7_{25}$ | $6_{24}$ | 325.72[b,f] | $8_{26}$ | 313.09[b,f] | -0.03 | -0.06 |
| $8_{27}$ | $7_{26}$ | 326.38[b,f] | $9_{28}$ | 312.03[b,f] | 0.01 | -0.01 |
| $9_{27}$ | $8_{26}$ | 327.26[c,f] | $10_{28}$ | 311.18[b,f] | 0.04 | 0.02 |
| $10_{29}$ | $9_{28}$ | 327.75[c,f] | $11_{2,10}$ | 310.02[b,f] | 0.02 | 0.00 |
| $11_{29}$ | $10_{28}$ | 328.43[c,f] | $12_{2,10}$ | 309.01[b,f] | -0.01 | -0.03 |

[a] Identified from supersonic expansion excitation spectra

[b] Identified by laser-induced fluorescence

[c] Assigned by ground state combination differences.

[d] Double entry $F_2(F_1)$ assigned by combination differences.

[e] Used in fitting molecular constants for the $K'_a = 1$ and 2 subbands of the 6125Å band

[f] Used in fitting molecular constants for the $K'_a = 0$, 1 and 2 subbands of the 6126Å band

in the 6125-Å region. If vibrational mixing (*3*) may be assumed negligible, the vibrational intensities suggest that the 6125-Å region is characterized by more quanta of $\nu'_1$ than is 5933 Å. Fluorescence to $n\nu''_2$ decreases more slowly with increasing $n$ in the 6126- and 6117-Å bands than in the 6119- and 6125-Å bands, implying that the bending vibrational mode may be more highly excited in the 6117- and 6126-Å bands than in the 6119- and 6125-Å bands. However, it should be noted that the observed vibrational progression is not sufficiently long to ensure the validity of these conclusions.

It is possible to determine whether the vibronic transitions originate from the vibrationless level of the ground state or from a "hot" band. At room temperature only the (0,1,0) ground state vibrational level is expected to have sufficient population to give rise to "hot" band transitions of readily detectable intensity in this spectral region. In fluorescence the occurrence of such a "hot" band transition would be indicated by the presence of fluorescence to a level displaced from the excitation frequency by $\nu_1'' - \nu_2''$ (~570.2 $cm^{-1}$) and by an anti-Stokes transition to a level located ~750 $cm^{-1}$ ($1\nu_2''$) above the excitation frequency. Careful examination of the low resolution spectra indicates that the 6119-, 6125-, and 6126-Å bands are "cold" bands and that the 6117-Å band is a "hot" band.[4]

The 6119-Å band exhibits a weak, structureless feature where fluorescence to $\nu_3''$ is expected; inspection of other bands reveals similar weak but reproducible features occurring at ~1630 $cm^{-1}$ below excitation. Fluorescence to odd quanta of $\nu_3''$ ($b_2$) from a totally symmetric ($a_1$) vibrational state is electronically forbidden, but vibronically allowed; thus, the ratio of the intensity of $\nu_2''$ (or $\nu_1''$) to the intensity of $\nu_3''$ may be interpreted as an estimate of the relative strength of electronically forbidden vibronically allowed transitions. For the 6119-Å band, fluorescence to $\nu_3''$ is about one-fifth as strong as fluorescence to $\nu_2''$ or $\nu_1''$; for the other bands considered, fluorescence to $\nu_3''$ is relatively weaker.

Several investigations of $NO_2$ (*14*) were severely hampered by an emission continuum superimposed on the discrete fluorescence. For excitation in the 6125-Å region, the presence of an emission continuum is not readily discernible when no correction for photomultiplier or spectrometer response is made (*15*).

Rotationally resolved fluorescence spectra were obtained by monitoring fluorescence to $2\nu_2''$. The $K_a$ value is determined from the $v_2K_a^2$ dependence of the ground state vibration–rotation interaction constants. Using available constants (*4*), the expression used to determine $K_a$ is

$$\Delta\nu(v_2'' = 2) \approx 1498.34 + 0.74K_a^2 \text{ cm}^{-1} \quad (1)$$

where $\Delta\nu$ ($v_2'' = 2$) is the resonance fluorescence frequency shift from excitation of a "fictitious" $Q$ branch transition from the vibrational ground state to the ($v_1'' = 0$, $v_2'' = 2$, $v_3'' = 0$) level.

Figure 4 shows rotationally resolved fluorescence spectra that illustrate the $K$ dependence. For $N'$ less than 8, it is possible to double the scan rate of the X–Y recorder and thus obtain a better determination of $K_a$. On the basis of the fluorescence spectra alone, it is not always possible to distinguish between $K_a' = 0$ and $K_a' = 1$, but the $K_a$ value can be determined by examining the combination differences and also the Fortrat diagram of the assigned transitions. The ground state energies and hence the combination differences were calculated using a complete matrix diagonalization doublet asymmetric rotor computer program and

[4] This conclusion is supported by the supersonic expansion excitation spectra (see Figs. 9 and 10). When the vibrational temperature is increased from ~150 to ~200 K, the 6117-Å band increases in intensity at a rate greater than that of the 6119- and 6125-Å bands; the latter all gain intensity at approximately the same rate. Furthermore, the 6117-Å band displays a similar pattern to the 5851-Å band which lies 750 $cm^{-1}$ to higher frequency (see Fig. 11): both the 5815- and 6117-Å bands appear to lack the higher frequency spin component of the $N' = 1$, $K_a' = 0$ P branch transition. Supersonic expansion excitation spectra of the 5851-Å band and of the 6125-Å region are also published in Refs. (*1* and *11*).

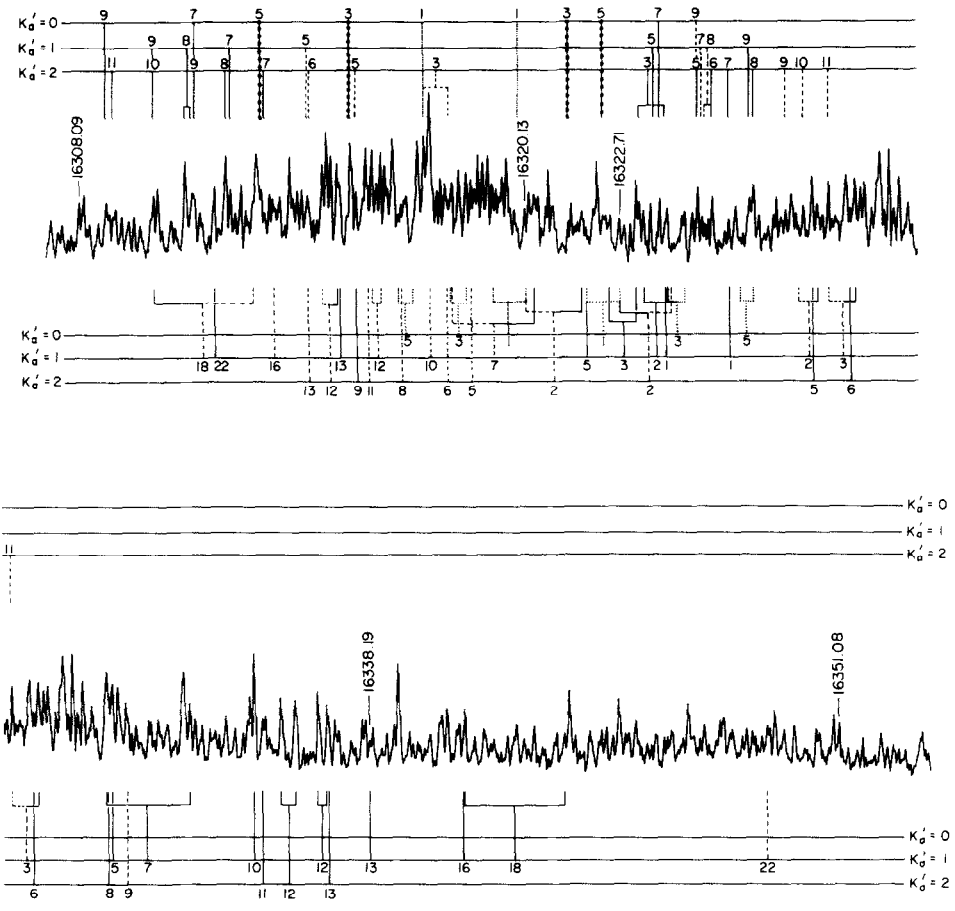


FIG. 5. Microdensitometer tracing of the $NO_2$ visible spectrum in the 6125-Å region. The excited state quantum number assignments are indicated above the tracing for the 6125-Å band and below the tracing for the 6125-Å band. Solid lines represent transitions assigned by laser induced fluorescence, dashed lines by combination differences, and dotted lines by analysis of supersonic expansion excitation spectra.

the ground state rotational constants of Hurlock *et al.* (*16*), as well as microwave-determined spin constants (*17*).

Figure 4 shows that the fluorescent $R$ and $P$ branch transitions have substantial intensity, but that the $Q$ branch transition is weak or missing. This emission line pattern is characteristic of $\Delta K = 0$ transitions. The vibronic symmetry of the upper state cannot be $B_1$ since $B_1$–$A_1$ transitions are expected to observe $\Delta K = \pm 1$ selection rules. The presence of $A_2$ vibronic levels can also be eliminated since they are only connected to the ground state by a magnetic dipole moment and the observed intensity is far too strong to be accounted for by such a transition. However, $B_2$ vibronic bands do obey $\Delta K = 0$ selection rules and are expected to have significant transition probability. Thus, the upper state vibronic symmetry is identified as $B_2$. This conclusion is supported by the absence of transitions to levels with even $N'$ in the $K_a' = 0$ subbands. This occurs because in $N^{16}O_2$

nuclear spin statistics allow only levels of $A_1$ or $A_2$ spinrovibronic symmetry to exist (*18*). If $C_{2v}$ symmetry is assumed, a $B_2$ (or a $B_1$) vibronic state can show such an alteration for $K_a = 0$. Moreover, since the transition strength indicates that the transitions are electronic symmetry allowed, the upper state vibration has $a_1$ symmetry and the electronic symmetry of the excited state must be $^2B_2$ for these vibronic bands.

In Table I we present listings of the line positions and their assignments for the bands in the $NO_2$ 6125-Å region.[5] Columns 6 and 7 contain the observed $R-P$ separation minus the calculated energy difference of the ground state ($N'' = N' - 1$, $K_a''$) and ($N'' = N' + 1$, $K_a''$) energy levels. The $F_1$ and $F_2$ headings refer to the two spin components $F_1(J = N + \frac{1}{2})$ and $F_2(J = N - \frac{1}{2})$. When the ground state spin splitting is sufficiently large, i.e., larger than the uncertainty due to line position measurement or blending, a unique assignment of a transition as either $F_1 \leftarrow F_1$ or $F_2 \leftarrow F_2$ is possible. This appears to be the case for the $K_a = 1, N' = 2$ and 3 transitions in the 6125-Å band. Inspection of the Fortrat diagram also allowed some spin component assignment to be made. In the cases where spin assignments are possible, the (obs − calc) value appears in the appropriate column and the other column is left blank. Spin component assignments could only be assigned in the $K_a' = 1$ and 2 subbands of the 6125-Å band; several $K_a' = 2$ transitions of the 6126-Å band exhibit large ground state spin splittings, but these transitions are found to be blended so the spin assignment is ambiguous. Discrepancies between the observed and calculated values, which are somewhat larger than the uncertainty in the line position measurements, are apparently due to the blending of lines. Dual entries occur in columns 3 and 5 when use of the method of combination differences does not yield unambiguous assignment of the line position of a transition.

In order to present the assignments of the overlapping 6125 and 6126-Å bands, Fig. 5 shows a microdensitometer tracing of this region, taken from the high resolution plates. The assignments of the 6125-Å band are distinguished from those of the 6126-Å band by indicating the quantum numbers beneath and above the tracing, respectively. Spin components are identified where possible. Inspection of these figures reveals that there still remains a number of unassigned sharp features which were not investigated.

No attempt is made to extend the analysis by classical methods beyond those transitions identified either by laser-induced fluorescence and their combination difference partner or by examination of the supersonic expansion excitation spectra.

The intensity distribution of the 6125-Å region bands appears to be more nearly Boltzmann than that of the 5933-Å band. At room temperature the peak intensity is expected to occur at $N' = 16$ and the $K_a' = 1$ subband is predicted to be the most intense subband. In the 5933-Å band the peak intensity occurs at $N' = 7$, and the intensity decreases with increasing $K_a$ more quickly than expected with $K_a' = 0$ being most intense (*8*). In the 6117- and 6119-Å bands the only transitions identified by laser-induced fluorescence occur for $K_a' = 0$ and 1 and $N'$ in

[5] These listings are more extensive than the preliminary analysis published in Hsu *et al.* (*1*). There have been changes in some of the assignments presented there; in particular, the band that is designated 6126 Å here is there designated as 6127 Å.

TABLE II

Observed Radiative Lifetimes for Selected $NO_2$ Transitions

| Band (Å) | $\nu$ ($cm^{-1}$) | $N'$ | $K_a'$ | $\tau_R$ ($\mu$sec) |
|---|---|---|---|---|
| 6117 | 16 361.69 | 19 | 0 | 65±6 |
| 6117 | 356.45 | 15 | 1 | 67±6 |
| 6117 | 329.94 | 15 | 1 | 55±6 |
| 6117 | 359.26 | 17 | 1 | 57±1 |
| 6117 | 359.53 | 17 | 1 | 57.5±1 |
| 6119 | 347.10 | 13 | 1 | 54±5 |
| 6119 | 348.15 | 15 | 1 | 73±7 |
| 6125 | 331.02 | 7 | 1 | 65.5±6 |
| 6125 | 333.27 | 7 | 1 | 53±5 |
| 6125 | 335.05 | 10 | 1 | 79±8 |
| 6125 | 337.03 | 12 | 1 | 81±8 |
| 6125 | 338.19 | 13 | 1 | 69±7 |
| 6125 | 343.54 | 18 | 1 | 75±7 |
| 6125 | 349.12 | 22 | 1 | 72±7 |
| 6125 | 331.14 | 8 | 2 | 79±8 |
| 6125 | 335.27 | 11 | 2 | 76±7 |
| 6125 | 335.76 | 12 | 2 | 82±8 |
| 6125 | 336.16 | 12 | 2 | 69±7 |
| 6125 | 337.08[a] | 13 | 2 | 81±8 |
| 6125 | 343.68 | 17 | 2 | 74.5±7 |
| 6126 | 310.02[a] | 9 | 1 | 71.5±7 |
| 6126 | 312.03 | 8 | 2 | 78.5±8 |
| 6126 | 311.18[a] | 9 | 2 | 65±6 |

[a] Transition may be blended.

the range 11 to 19; $K_a' = 1$ transitions are stronger than the $K_a' = 0$ transitions. In the $R$ branch of the 6117-Å band, the $K_a' = 1$ transitions appear to be about twice as strong as the $K_a' = 0$ transitions. In the 6125-Å band the peak of the intensity distribution occurs in the vicinity of $N' = 14$ and transitions up to $N' = 22$ have been identified; however, there is substantial variation in intensity from one $N'$ transition to the next. In the 6125-Å $K_a' = 0$ subband only one transition ($N' = 3$) has been identified by laser-induced fluorescence; because of the extensiveness of this study, this suggests that the intensity of the 6125-Å $K_a' = 0$ subband decreases more rapidly than for other $K$ subbands of the 6125-Å band. In the 6126-Å band the $K_a' = 0$, 1, and 2 subbands appear to exhibit roughly comparable intensities; the peak intensity occurs at about $N' = 7$ and falls rather rapidly with 11 being the highest $N'$ value observed. Three $K_a' = 3$ transitions were observed, but are not reported here because of ambiguities in the data; their intensities are weaker than that of $K_a' = 1$ and 2 subbands of this region.

About a half-dozen transitions were identified that could not be associated with any of the four vibronic bands whose transitions dominate this region, e.g., both the $11_{1,10} \leftarrow 10_{19}$ transition at 16 340.16 $cm^{-1}$ and the corresponding $11_{1,10} \leftarrow$

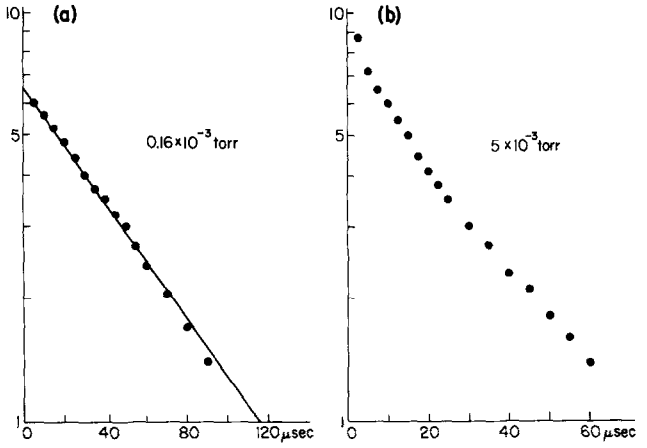


FIG. 6. Plot of the logarithm of the fluorescent intensity ($\nu$(ex) = 16 338.19 cm$^{-1}$) versus time (a) at 0.16 mTorr and (b) at 5 mTorr.

$12_{1,11}$ transition at 16 320.50 cm$^{-1}$ were identified by laser-induced fluorescence, but the transitions lie about 4 cm$^{-1}$ to higher frequency of where the $N' = 11$, $K_a' = 1$ transition of the 6125-Å band is expected and about 6 cm$^{-1}$ to lower frequency of the 6119-Å band position.

### *B. Lifetime Measurements*

Using the experimental arrangement described in Section II, the radiative lifetimes $\tau_R$ of 23 isolated transitions are measured at pressures of $\leq$1 mTorr and are presented in Table II. As shown in Fig. 6a, single exponential decay is observed at pressures $\leq$1 mTorr while at pressures of 5 mTorr and greater, the radiative decay is nonexponential (Fig. 6b). At 5 mTorr when fluorescence to 1 $\nu_2''$ is moni-

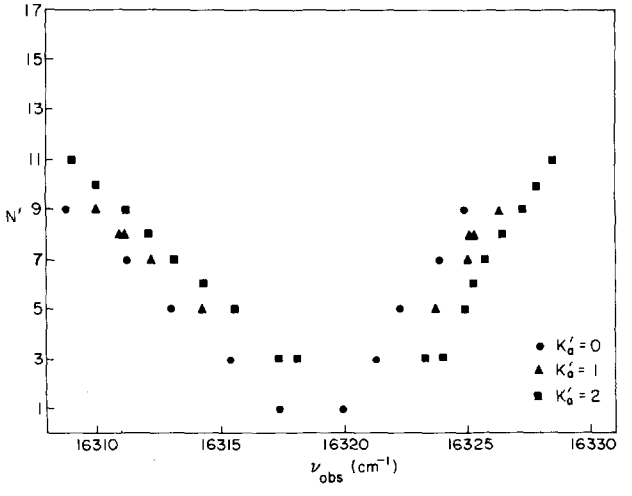


FIG. 7. Modified Fortrat diagram of the $NO_2$ 6126-Å band.

TABLE III

Derived Upper State Molecular Constants for the $NO_2$ 6125-Å Region

| | | | |
|---|---|---|---|
| $\nu_0$ | 16 319.30 $cm^{-1}$ [a,b] | 16 327.31 $cm^{-1}$ [b,c] | 16 326.93 $cm^{-1}$ [d] |
| A | 8.47 | 7.03 | 7.15 |
| $\bar{B}$ | 0.390 | 0.432 | 0.4417 |
| B | 0.420 | 0.46 | 0.456 |
| C | 0.360 | 0.41 | 0.427 |
| $D_N$ | $-1.2 \times 10^{-4}$ | $-4 \times 10^{-5}$ | $2.9 \times 10^{-5}$ |
| $\epsilon_{aa}$ | | | 0.95 |
| $\bar{\epsilon}$ | | | 0.047 |
| $\Delta$ | 4.70 amu-$Å^2$ | 2.40 amu-$Å^2$ | 0.15 amu-$Å^2$ |
| $\sigma$ | 0.21 $cm^{-1}$ | 0.16 $cm^{-1}$ | 0.18 $cm^{-1}$ |

[a] For $K_a' = 0, 1$, and 2 of $NO_2$ 6126Å band.

[b] The mean of the line positions is included in the fitting program; however, for several rotational transitions only one of the spin components is assigned, and its line position is entered as the location of $F_1$ and $F_2$.

[c] For $K_a' = 1$ and 2 of $NO_2$ 6125Å band, using mean of the spin splittings.

[d] For $K_a' = 1$ and 2 of $NO_2$ 6125Å band.

tored through the 1-m spectrometer with 2-mm slit width, we again detect single exponential radiative decay. This suggests that in the 6125-Å region the nonexponential behavior we observe is due to collisional transfer of energy. In order to test this hypothesis, a brief study of fluorescence quenching with Ar and with $NO_2$ itself using pressures in the range 0–10 mTorr is performed. Quenching of $NO_2$ fluorescence by collisions with Ar is found to be characterized by a collision cross-section of 12 $Å^2$ and occurs at a rate of $0.69 \times 10^7$ $sec^{-1}$ $Torr^{-1}$, while the cross section is 35 $Å^2$ and the quenching rate is $0.95 \times 10^7$ $sec^{-1}$ $Torr^{-1}$ for collisional quenching of $NO_2$ by itself. The $NO_2$ self-quenching constant yields a collision diameter of 5.1 Å. However, this result implies that at 5 mTorr an $NO_2$ molecule experiences a collision every 60 $\mu$sec on the average. If Fig. 6b is assumed to display biexponential decay, then at 5 mTorr the apparent lifetime of the shorter component is ~25 $\mu$sec and of the longer component ~40 $\mu$sec. From the available data, it is not clear whether the nonexponential behavior may be accounted for by collisional quenching or whether the radiative decay is nonexponential even at pressures $\leq 1$ mTorr. The latter possibility might escape detection at such pressures because the decay is not monitored over a sufficiently long time interval, because the intensity of the long-lived component is weak, and/or because of geometric factors (*19*).

Stevens *et al.* (*7*) reported biexponential decay in the 5933-Å region when the laser was tuned to a rotational transition; however, they observed only the longer

lifetime when the laser was tuned between rotational transitions. This observation has been confirmed by Donnelly and Kaufman (*20*). In the 6125-Å region we have searched for fluorescence when the laser is tuned between transitions and we have been unable to detect measurable fluorescence.

Donnelly and Kaufman (*20*) have observed nonexponential radiative decay in the $NO_2$ 5780–6130-Å region, using pressures of 0.01 to 25 mTorr. Assuming the radiative decay is biexponential, they find linear Stern–Volmer plots at all pressures studied for the shorter radiative lifetime $\tau_S$. For the longer radiative lifetime $\tau_L$, the Stern–Volmer plots deviate from linearity at low pressure. In the 6125-Å region the unweighted average of the $\tau_S$ lifetimes is 52 and 208 $\mu$sec for $\tau_L$ as determined from the "high pressure" linear portion of the Stern–Volmer plot. These may be compared with the radiative lifetimes obtained in this study. Excitation at 6123.2 Å with a 0.5-Å bandwidth accesses both the $R$ branch transitions of the 6125-Å band and the bandhead of the 6117-Å band. Thus, the $\tau_S$ observed by Donnelly and Kaufman at 6123.2 Å may be attributed to the 6117-Å band. The nonlinearity of the Stern–Volmer plots at low pressure *might* account for the discrepancy between Donnelly and Kaufman's low pressure $\tau_L$ (~90 $\mu$sec) and the radiative lifetime of the 6125-Å band obtained in this study (~70 $\mu$sec).

## IV. ANALYSIS AND DISCUSSION

### A. *The 6125- and 6126-Å Bands*

The $K_a' = 0$, 1, and 2 subbands of the 6126-Å band and the $K_a' = 1$ and 2 subbands of the 6125-Å band are fit to the energy expression of an asymmetric top. We use a computer program based upon the asymmetric rotor formulations of Raynes (*21*) and including matrix elements for $|\Delta K| \leq 2$ and $|\Delta N| \leq 1$. The rotational and spin constants are adjusted iteratively to obtain a least squares fit to the observed line positions. The upper state constants are free to vary; the ground state rotational constants are fixed to values obtained from infrared studies (*16*) and ground state spin constants to those from microwave studies (*17*). The parameters $\nu_0$, $A' - \bar{B}'$, $\bar{B}'$, $(B' - C')$, and $D_N'$ are simultaneously fit; for $K_a' = 1$ and 2 of the 6125-Å band, $\epsilon_{aa}$ and $\bar{\epsilon}$ are also included in the fit. Given the prevalence of the perturbations in $NO_2$ and the high covariance among the constants obtained, it is felt that more parameters could not be meaningfully determined.

Figure 7 presents a modified Fortrat diagram of the 6126-Å band. The band appears to be well behaved with very few local perturbations. A straight line may be passed through most of the $R$ (or $P$) branch member of each $K$ subband; this suggests that either the spin splittings are small or that one spin component in a given $K$ subband is appreciably weaker than the other. Careful examination reveals that (1) the $J$ structure degrades to the red with a bandhead expected in the $R$ branch at $N' = 13$, and (2) the $K$ structure degrades to the blue. The directions of degradation of the $J$ and $K$ structures imply that the "equilibrium" bond angle is larger in the excited state than in the ground state (*22*); this suggests that the 6126-Å band has a large amount of ground state character, since the bond angle of the $^2B_2$ state is smaller than that of the ground state (*8, 10, 12*) and since

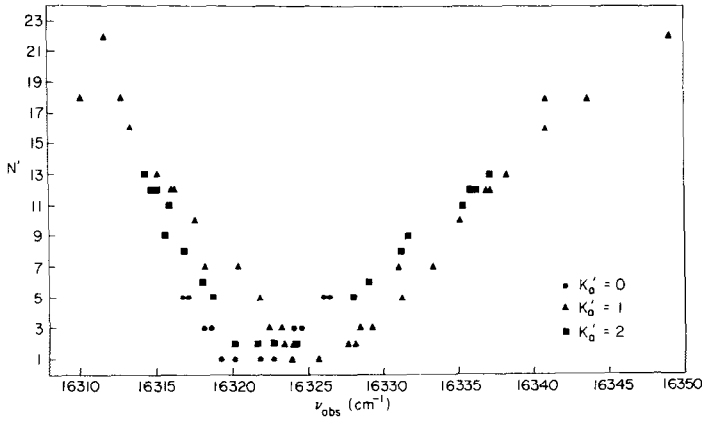


FIG. 8. Modified Fortrat diagram of the $NO_2$ 6125-Å band.

the "equilibrium" bond angle of ground state vibrational levels increases until the barrier to linearity is reached.

Column 2 of Table III presents the constants obtained from fitting $K_a' = 0$, 1, and 2 of the 6126-Å band. The inertial defect $\Delta$ is rather sizeable, but large inertial defects have been reported for other $NO_2$ bands (*8*, *10*, *23*). What is even more disturbing is that the centrifugal distortion constant $D_N$ is negative. Interaction with other levels can cause exotic apparent centrifugal distortion effects: for example, one component of the (0,11,0) $\Sigma$ level of the $CS_2{}^3A_2(\Delta_u)$ $R$ state may be characterized by a negative centrifugal distortion constant while the other two components display normal centrifugal distortion, but are significantly perturbed as evidenced by missing $J$ levels (*24*). A complementary explanation is obtained by examining the effect of spin assignments in the fit of the 6125 Å band. Column 3 of Table III lists the molecular constants obtained from fitting $K_a' = 1$ and 2 of the 6125-Å band when the mean of the spin splittings are used. Again, $D_N$ is negative and $\Delta$ is large. Column 4 of Table III presents the constants obtained from fitting $K_a' = 1$ and 2 of the 6125-Å band when spin components are assigned. Here $D_N$ is positive and $\Delta$ is unusually small for an $NO_2$ excited state band. Thus, the negative $D_N$ of the 6126-Å band may in part arise from the inability to assign spin components. This may also partially explain the large inertial defect found in the fit.

Inspection of Columns 3 and 4 of Table III also reveals that the $A$ and $\bar{B}$ constants differ by 2% and the other constants display slightly larger variations. The latter occurs because of the way spin components are entered into the fit (see footnote b of Table III). Consequently, the Fortrat parabola is "tilted" slightly and the derived constants slightly modified.

The ground state value of $D_N$ is $\sim 2.8 \times 10^{-7}$ cm$^{-1}$ (*16*), while the $D_N$ values reported in Table III and by other researchers (*8*, *10*) are of the order of $10^{-5}$ cm$^{-1}$. This difference in magnitude may result in part from the effects of perturbations, and from absence of any other centrifugal distortion constants in the fit. Thus $D_N$ should be considered as an effective centrifugal distortion constant.

Figure 8 presents a modified Fortrat diagram of the 6125-Å band. Several spin splitting pairs have been assigned, and the spin splitting is sufficiently large that spin components may often be assigned from inspection of the Fortrat diagram when only one of the spin splittings is known. The $\bar{\epsilon}'$ value determined is of the expected magnitude, but the $\epsilon'_{aa}$ value is slightly large: one anticipates that $\epsilon'_{aa}$ will be of the order of the ground state value (0.18 $cm^{-1}$). In contrast to the 6126-Å band, the $J$ structure degrades to the blue with the bandhead in the $P$ branch at $N' \simeq 21$ and the $K$ structure (for $K'_a = 1$ and 2) degrades to the red. This suggests that the "equilibrium" bond angle is smaller than in the ground state (*22*). This implies that the 6125-Å vibronic band has predominantly the character of the $^2B_2$ excited state.

Although the 6125-Å $K'_a = 1$ and 2 subbands appear well behaved, the $K'_a = 0$ subband is decidedly perturbed (see Fig. 8) while $K'_a = 0$ of the 6126-Å band seems normal. The subband origin of $K'_a = 0$ in the 6125-Å band is found about 5.5 $cm^{-1}$ to lower frequency of where it is expected to be located, based on analysis of the $K'_a = 1$ and 2 subbands. Furthermore, there is a perplexing spin perturbation. Since we are unable to make spin assignments, the spin component at lower energy is labeled $a$ and the spin component at higher energy is assigned the label $b$ (*25*). The $b$ spin components were fit to

$$\nu = 16\,321.81 + 0.434N'(N' + 1)\ cm^{-1} \tag{2}$$

with (obs − calc) of the order at 0.01 $cm^{-1}$ while the $a$ spin components were fit to

$$\nu = 16\,320.99 + 0.449N'(N' + 1)\ cm^{-1} \tag{3}$$

with (obs − calc) of the order of 0.11 $cm^{-1}$. The residuals suggest that the $a$ spin components may be more perturbed than the $b$ spin components. Moreover, this conclusion is supported by the observation that the spin splitting is observed to *decrease* from 0.90 $cm^{-1}$ for $N' = 1$ to 0.42 $cm^{-1}$ for $N' = 5$ although spin splittings for $K = 0$ subbands are expected to be described to a good approximation by

$$(F_1 - F_2) = \bar{\epsilon}'(N' + \tfrac{1}{2}). \tag{4}$$

The origin of the $K'_a = 0$ perturbation(s) is uncertain. The perturbation must have a $K$ dependence and appears to affect one spin component more than the other. In order to understand the observed perturbations, we have investigated the effects of Renner–Teller interaction, spin–orbit coupling, Coriolis interaction, Fermi interaction, and vibronic coupling (*27*). Although none of these mechanisms can account satisfactorily for the observed spin perturbations, we have arrived at an explanation of the other observations. Examination of the sense of the asymmetry staggering eliminates Renner–Teller interaction and also spin–orbit coupling as possible sources of the perturbation (*28*). Coriolis interaction may be discarded on the basis of symmetry considerations. Both Fermi interaction and vibronic coupling must be invoked to explain the major features of this region.

The origins of the 6125- and 6126-Å bands lie within 10 $cm^{-1}$ of each other. It would therefore be surprising if these two bands did not interact to some extent. As noted previously, the $J$ and $K$ structures of the 6125-Å band degrade in

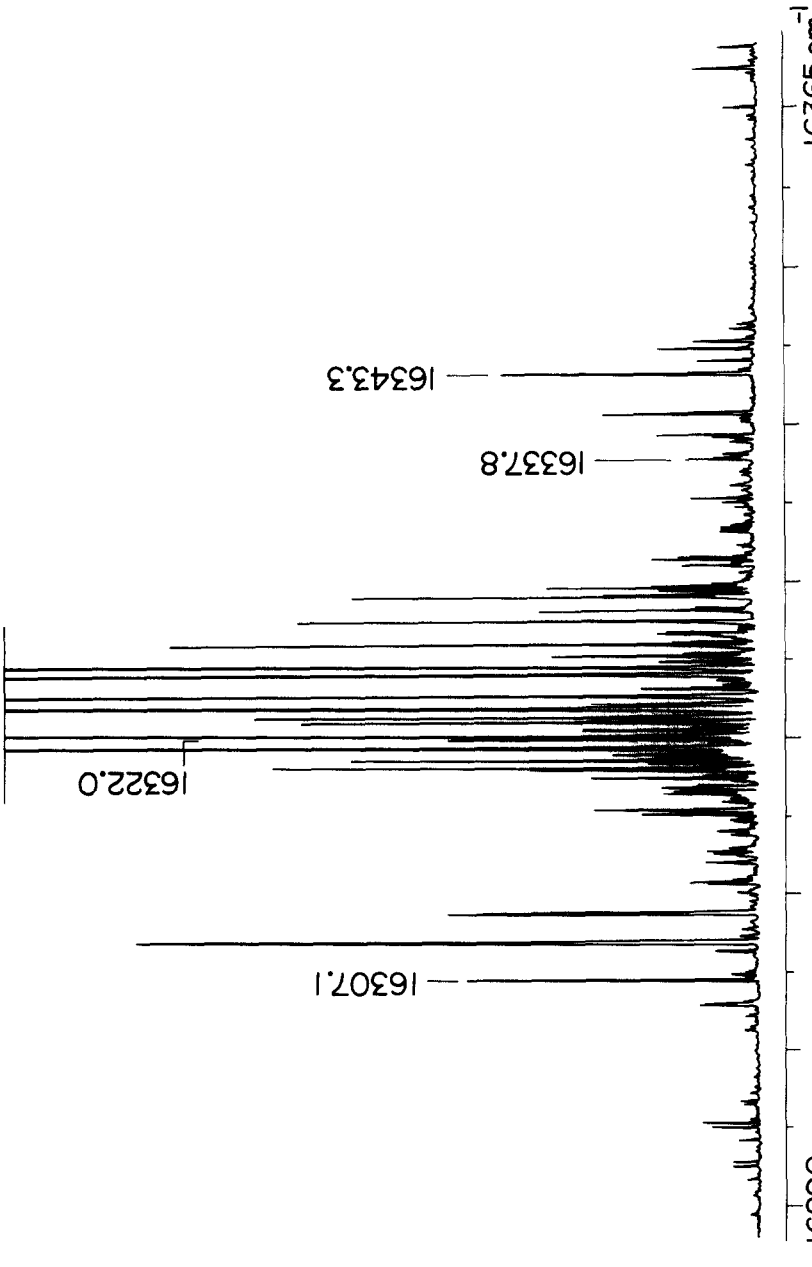


FIG. 9. Supersonic expansion excitation spectrum of the $NO_2$ 6125-Å region, adapted from Smalley *et al.* (*26*). The rotation temperature $T_{rot}$ is about 3 K and the vibrational temperature $T_{vib}$ about 200 K.

opposite directions to those of the 6126-Å band. Since the 6125-Å band has more excited state character and the 6126-Å band more ground state character, the opposite directions in these two bands suggest that the 6126-Å band is induced by a repulsive (Fermi) interaction with the 6125-Å band. Assuming that the two bands were initially degenerate and are shifted to the observed positions by a simple Fermi interaction, the modified Fortrat diagram presented in Fig. 12 is obtained. The $K'_a = 1$ and 2 subbands again appear well behaved. The molecular constants for $K'_a = 1$ and 2 are the mean of the two bands: $A' = 7.8\ \text{cm}^{-1}$, $\bar{B}' = 0.42\ \text{cm}^{-1}$. These compare favorably with those obtained for the 5933-Å band (*8*, *9*, *30*): $A' = 7.85\ \text{cm}^{-1}$, $\bar{B}' = 0.4224\ \text{cm}^{-1}$.

The effects of Fermi interaction may be manifested in the spin perturbations of this region. In the 6126-Å band it appears that either the spin splittings ($F_1 - F_2$) are small or only one spin component is observed. The spin splittings of the 6125-Å $K'_a = 1$ and 2 subbands are large and the spin splitting pattern fairly well established. Examination of supersonic excitation spectra (*1*, *11*) clearly shows that the *a* spin components of the 6125-Å $K'_a = 0$ subband are significantly more intense than the *b* components. If the 6125- and 6126-Å bands are "mirror images," one expects to observe the same spin splitting in both bands and the *b* spin components of the 6126-Å band stronger than the *a* spin components.[6] Careful inspection of the supersonic expansion excitation spectra does not enable us to resolve this question since the intensity of the *b* spin components of the 6126-Å band is so weak, and that of the *a* spin components is comparable to the background noise.

The extent and pervasiveness of vibronic coupling in $NO_2$ has been dramatically documented by the supersonically cooled spectra of Smalley, *et al.* (*1*, *11*). This interaction is between a few excited state levels (one of which probably carries most of the oscillator strength) and several ground state levels. Before the perturbation is "turned on," the *A* values of the excited state levels are about $2.8\ \text{cm}^{-1}$ (*10*, *12*) and those of the ground state are of the order of 5 times larger. Merer (*31*) has suggested that since there is no rotational quantum number dependence, each *K* stack should be treated as a separate case. That is, each *K* stack in the excited state manifold and in the ground state manifold effectively interacts with a different "environment" than the other *K* stacks of the same vibrational level; local effects may cause relative shifting of some *K* stacks within a vibrational band.[7] This mechanism thus accounts for the appearance of the 6126-Å band and the reordering of the 6125-Å $K'_a = 0$ stack, but does not explain the "mirror image" relationship between the 6125- and 6126-Å bands nor the spin splitting perturbations.

We conclude that the most likely explanation for the appearance of the 6125- and 6126-Å bands is a combination of Fermi interaction and vibronic coupling. Fermi interaction accounts for the "mirror image" behavior, but cannot account for the 6125-Å $K'_a = 0$ subband shift of several wavenumbers from its expected

[6] Mirror symmetry for the spin splitting would not hold if the 6126-Å band were an induced band and the perturbation that gave the 6125 Å its oscillator strength had an $F_1$ (or $F_2$) dependence.

[7] Brand *et al.* (*32*) have independently proposed this mechanism to account for the observed perturbations in the $NO_2$ 6480-Å region, where each *K* subband must be fit separately.

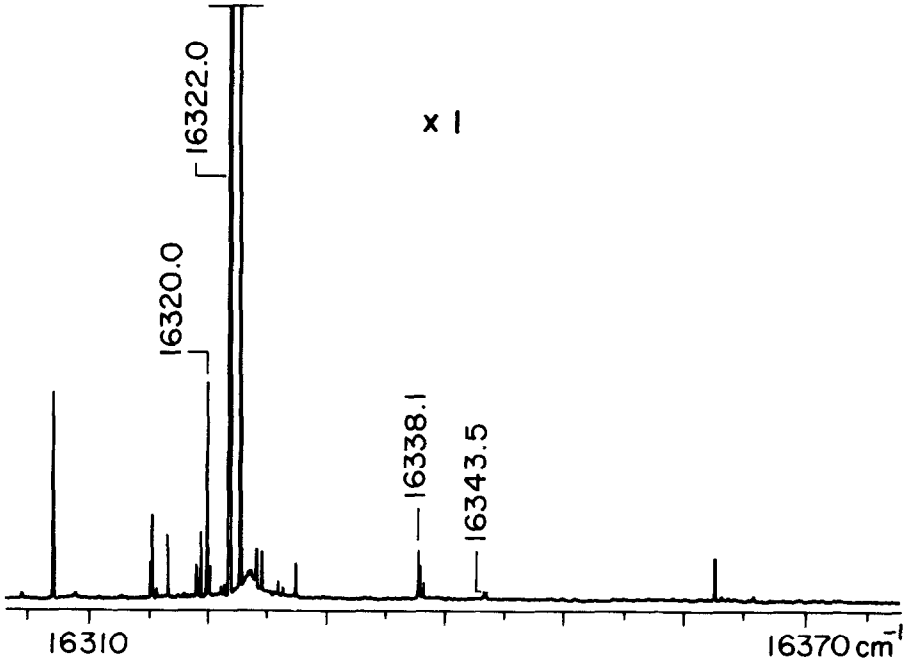


FIG. 10. Supersonic expansion excitation spectrum of the $NO_2$ 6125-Å region, adapted from Smalley *et al.* (*26*). $T_{rot} \simeq 0.5$ K, and $T_{vib} \simeq 150$ K.

position (see Fig. 12). Vibronic coupling can, however, explain the $K_a' = 0$ shift and the relatively well-behaved nature of the 6125-Å $K_a' = 1$ and 2 subbands. But the spin splitting perturbations cannot be attributed to either of these mechanisms.

### *B. The 6117- and 6119-Å Bands*

Because of the limited number of assignments (see Table I), few conclusions can be drawn about these bands. As mentioned previously, the 6117-Å band is a hot band transition that corresponds to the 5851-Å band. The $J$ structure of the 6117-Å band degrades to the blue and the $K$ structure degrades to the red, implying that the excited state bond angle is smaller than in the ground state (*22*). The upper state term values are fit to:

$$\text{for } K_a' = 0: \quad \nu = 16\,342.44 + 0.430N'(N' + 1)\ \text{cm}^{-1}, \tag{5}$$

$$\text{for } K_a' = 1: \quad \nu = 16\,346.04 + 0.449N'(N' + 1)\ \text{cm}^{-1}. \tag{6}$$

From these origins an $A'$ value of 3.2 $\text{cm}^{-1}$ is extracted. The $A'$ value is surprising in that it is of the expected magnitude of the unperturbed $A$ value of the $^2B_2$ state (*10, 12*). However, it is not clear whether the derived $A'$ value is a reasonable estimate of the "true" $A'$ value, because of the limited number of transitions. The spread in the $N'$ values in the $K_a' = 1$ subband is too small to permit determination of $D_N'$ and the observed data are fit with residuals on the order of 0.06 $\text{cm}^{-1}$. For the $K_a' = 0$ subband, the residuals of Eq. (5) are fairly

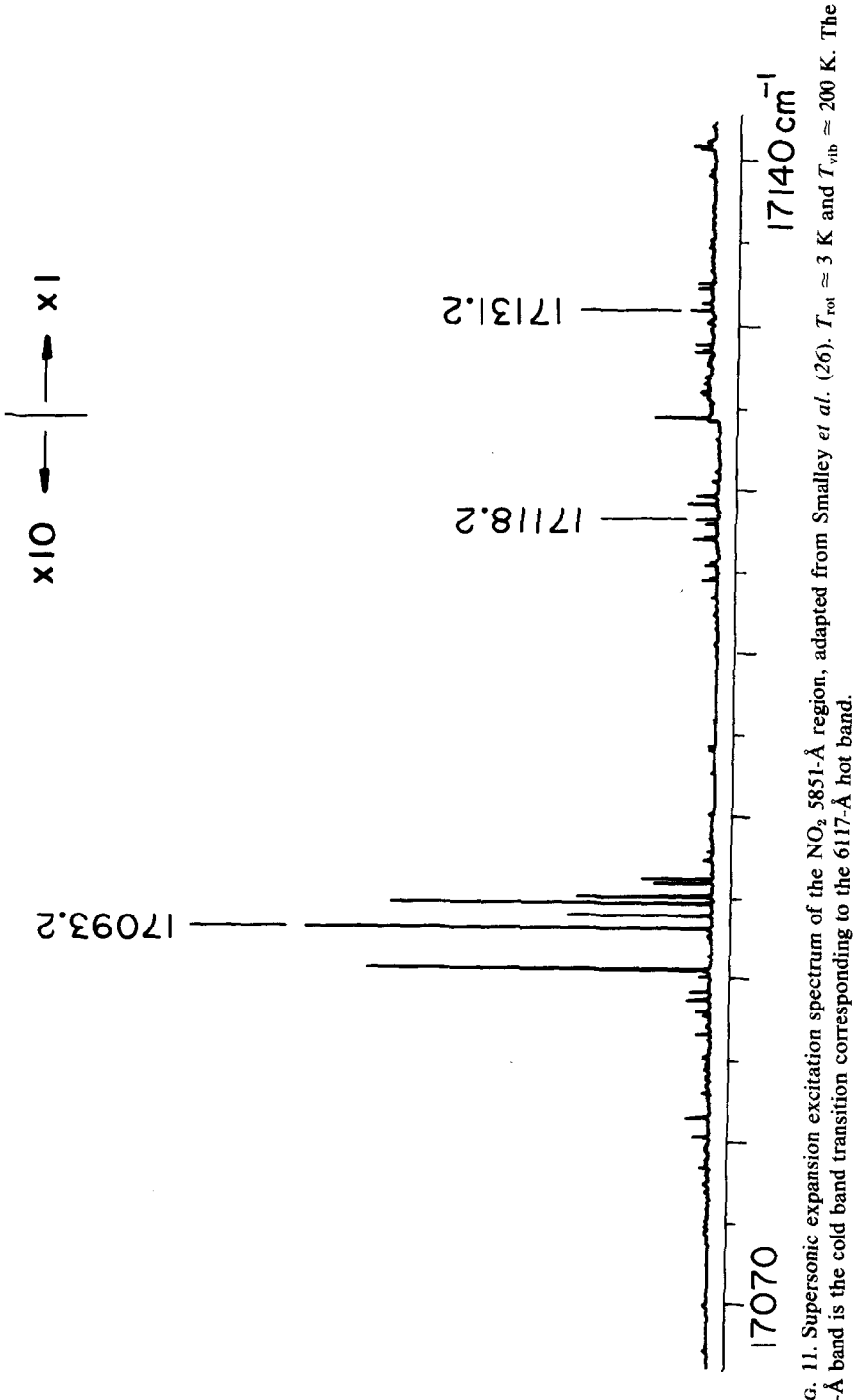


FIG. 11. Supersonic expansion excitation spectrum of the $NO_2$ 5851-Å region, adapted from Smalley *et al.* (26). $T_{rot} \simeq 3$ K and $T_{vib} \simeq 200$ K. The 5851-Å band is the cold band transition corresponding to the 6117-Å hot band.

large (0.28 $cm^{-1}$). Since the variation in $N'$ values is more extensive for $K'_a = 0$, we are able to fit the $K'_a = 0$ data to

$$\nu = 16\,342.41 + 0.4322N'(N' + 1) - 5.35 \times 10^{-6}[N'(N' + 1)]^2 \text{ cm}^{-1} \quad (7)$$

but the average residual is still 0.27 $cm^{-1}$. Like the 6125-Å band, the supersonic expansion excitation spectra (see Figs. 9 and 11) indicate that the $a$ spin component is substantially stronger than the $b$ component, and that the spin splitting *decreases* with increasing $N'$.

The $K'_a = 1$ subband of the 6119-Å band is fit to

$$\nu = 16\,345.17 + 0.419N'(N' + 1) \text{ cm}^{-1} \quad (8)$$

with an average residual of 0.14 $cm^{-1}$. The $J$ structure degrades to the red. The $K$ structure also appears to degrade to the red, but this observation is based on Eq. (8) and on the $K'_a = 0$ assignments from the supersonic expansion excitation spectrum; the situation is ambiguous because it is not certain whether Eq. (8) yields the "true" $K'_a = 1$ subband origin. Both the $J$ and $K$ structures degrading to the red implies that the bond length in the excited state is longer than in the ground state (*22*). If Eq. (8) provides a reasonable estimate of the $K'_a = 1$ subband origin, then an $A'$ value of 7.8 $cm^{-1}$ is obtained.

The assignments made by laser-induced fluorescence are matched to those from the supersonic excitation spectra[8] by assuming that the two sets smoothly join and by then matching the Fortrat diagram slopes of the assigned transitions.

### C. *Other Vibronic Bands in the 6125-Å Region*

Examination of the supersonic expansion excitation spectra (Figs. 9 and 10) confirms the presence of the four bands previously discussed. Moreover, four bands [6110 Å, $\nu(R_0(0)) = 16\,362.55$ $cm^{-1}$; 6127 Å, $\nu(R_0(0)) = 16\,316.70$ $cm^{-1}$; 6128 Å, $\nu(R_0(0)) = 16\,315.33$ $cm^{-1}$; and 6131 Å, $\nu(R_0(0)) = 16\,306.98$ $cm^{-1}$] appear in these spectra that we were unable to detect. Although transitions appear fairly strong in the excitation spectra, their absorption at room temperature is relatively weak. The cause of this discrepancy is unknown. However, the excitation spectra show that the 6125-Å band (having more excited state character) is much stronger than the 6126-Å band (see Fig. 10).

### D. *$NO_2$ Vibronic Bands with Similar Spin Perturbations*

The $K'_a = 0$ subband of the 6125-Å band displays a spin perturbation that causes the spin splittings to decrease with increasing $N$ (see Figs. 8–10). Similar spin

[8] In the 6125- and 6126-Å bands the assignments made by laser-induced fluorescence are matched with those from the supersonic expansion excitation spectra by the observation in both spectra of four $K'_a = 0$ transitions of the 6126-Å band and one $K'_a = 0$ transition of the 6125-Å band. Identification of $K'_a = 0$ transitions in the 6117- and 6119-Å bands is based on the fact that although the accuracy of the absolute frequency of the supersonic excitation spectra is ±0.2 $cm^{-1}$, the precision of the relative displacements is ±0.02 $cm^{-1}$.

The line positions given in Figs. 9–11 are based on the frequencies determined by Smalley *et al.* (*11*). The $R_0(0)$ line positions listed in Section IV.C were determined by utilizing transitions identified both by laser-induced fluorescence and in the excitation spectra, and by taking advantage of the ±0.02 $cm^{-1}$ precision of relative displacements in the excitation spectra; the transition is assigned to the $NO_2$ line found within ±0.02 $cm^{-1}$ of the calculated position.

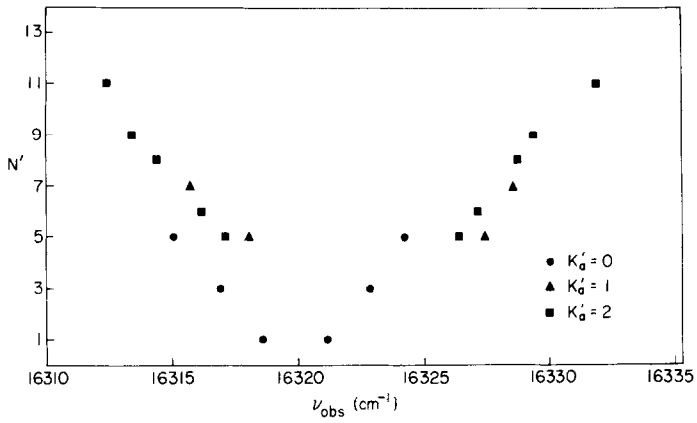


FIG. 12. Modified Fortrat diagram of the "deperturbed" 6125- and 6126-Å bands. The line positions plotted here are fictitious line positions representing the mean of the line positions in the 6125- and 6126-Å bands.

splitting behavior has also been reported by Merer and Hallin (*33*) for the $NO_2$ 8920-Å $K_a' = 0$ subband; furthermore, for part of this subband only one spin component was located. Thus the spin perturbation of the $K_a' = 0$ subband is not unique to the 6125-Å band.

Within 10 cm$^{-1}$ of the 6125-Å band appears a weaker band (6126 Å) that seems to be the mirror image of the 6125-Å $K_a' = 0$ subband. A careful search of supersonic expansion excitation spectra has uncovered other vibronic bands that (1) exhibit decreasing spin splittings with increasing $N$ (like the 6125-Å $K_a' = 0$ subband) and (2) near which can be found a weak vibronic band analogous to the 6126-Å band. They are located at 14 969.9, 15 252.5, 15 571.5, 17 092.3 (see Fig. 11), and 17 477.7 cm$^{-1}$ (see Fig. 13). The identification of these bands encourages us that a pattern in the perturbation does occur in the $NO_2$ visible spectrum.

Since a recurring pattern has been found, it is tempting to try to extract excited state vibrational frequencies. The meaning of such "frequencies" is made ambiguous by the fact that the supersonic expansion excitation spectra reveal that the $NO_2$ visible spectrum is replete with spin perturbations: for example, the 15 380.2-, 16 217.5- (*1*), 16 917.6- (*1*), and 17 400.9-cm$^{-1}$ bands exhibit spin splittings of constant magnitude while the 15 325.0-, 15 525.4-, and 16 578.1-cm$^{-1}$ bands (*1*) display spin splittings that increase "too quickly" with increasing $N$. The extensiveness and variety suggest that investigations of the spin perturbations in the $NO_2$ visible spectrum will contribute much to an understanding of the notorious complexity of this system.

### *E. Analysis of the $NO_2$ 6125-Å Region by Lee and Peck*

Recently a rotational analysis of the $NO_2$ 6125-Å region has been published by Lee and Peck (*1*, *34*). They report 21 experimentally assigned transitions; no assignments were made on the basis of combination differences. They assumed that all the assigned transitions arise from a single vibronic band.

Lee and Peck were severely hampered by wavelength calibration difficulties:

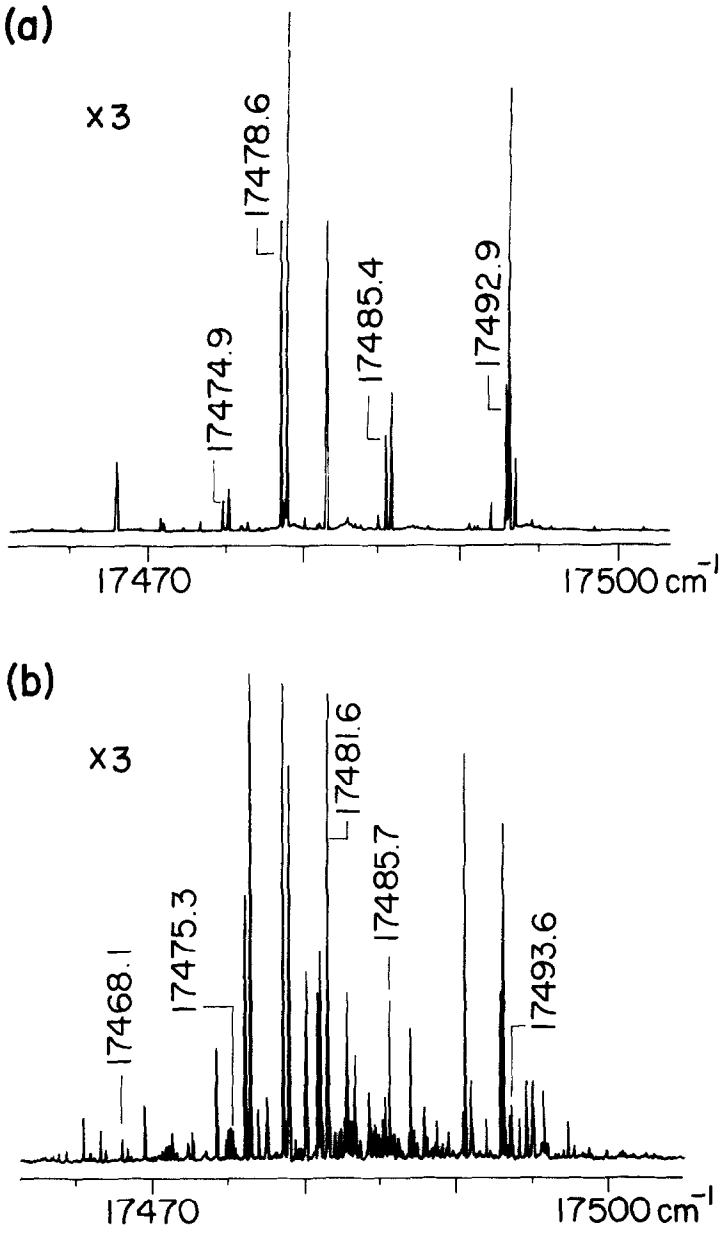


FIG. 13. Supersonic expansion excitation spectra of the $NO_2$ 5721 Å region: (a) $T_{rot} \simeq 0.5$ K, $T_{vib} \simeq 150$ K; and (b) $T_{rot} \simeq 3$ K, $T_{vib} \simeq 200$ K, adapted from Smalley *et al.* (*26*). The 17 474.2-$cm^{-1}$ band is the daughter of the band of the 17 478.0-$cm^{-1}$ band.

during the course of their investigation, Lee and Peck discovered that the performance of their spectrometer was erratic, leading to errors of several $cm^{-1}$ (*34*). If the quantum number assignments of both studies are assumed correct, the average difference between the line positions is found to be 1.58 $cm^{-1}$ for

$K'_a = 1$ (7 transitions) and 2.76 $cm^{-1}$ for $K'_a = 2$ (12 transitions). Alternatively, if the transitions are paired by similar line positions and similar quantum numbers, the average difference in the line positions is 0.50 $cm^{-1}$; this difference is of the same magnitude as the nominal precision of their spectrometer. Consequently, we are unable to use Lee and Peck's data in combination with our own to extend our analysis.

### *F. Vibrational Assignment of 6125-Å Bands*

A tentative vibrational analysis of the $NO_2$ 5930–11 500-Å region has been proposed by Brand *et al.* (*5*). That study and the subsequent analysis of the 8000–9000-Å region (*10*) locate the $^2B_2$ origin at 8357 Å . Thus, the 16 314-$cm^{-1}$ peak is attributed to the (2,0,1) ← (0,0,0) transition. However, the *ab initio* calculations of Gillespie *et al.* (*12*) and the recent analysis of the 8920-Å band by Merer and Hallin (*33*) place the $^2B_2$ origin at 10 250 Å. Based on their previously generated potential surfaces (*12*), Gillispie and Khan (*35*) have attempted to correlate the low resolution spectrum of the 6000–9000-Å region with their calculated band positions; they associate (1,7,0) ← (0,0,0) with the most prominent peak in the 6125-Å region.

The results of this study appear to be consistent with the assignment of Gillispie and Khan, but not with that of Brand *et al.*: the intensity of the fluorescence implies that the transition is electronically allowed and therefore $v'_3$ must be even. However, if the $\tilde{A}^2B_2$ and $\tilde{X}^2A_1$ states are so completely mixed that it is not meaningful to ascribe parentage to vibronic bands, then the terms "vibronically allowed" and "electronically allowed" are not applicable.

## V. CONCLUSION

The technique of laser-induced fluorescence provides an incisive probe of the $NO_2$ 6125-Å region. These results as augmented by those of supersonic expansion excitation spectroscopy have yielded a description of the rotational structure and perturbations in this complex region that is not attainable by classical methods. We have succeeded in assigning approximately 135 transitions. We find that as a whole the rotational structure of the four vibronic bands observed in this region appears well behaved and may be characterized by near-prolate symmetric top relations. The relative absence of rotational perturbations in the $NO_2$ 6125-Å region implies that strong vibrational perturbations are the cause of the complexity of this region. Perturbations in the 6125 and 6126-Å bands are well established; the most probable source appears to be a combination of Fermi interaction and vibronic coupling, although these cannot account entirely for the observations. Similar perturbations are found to recur in other $NO_2$ vibronic bands in the visible region; this discovery encourages us that a perturbation pattern does exist in the $NO_2$ visible spectrum.

## ACKNOWLEDGMENTS

We thank Richard Smalley, Lennard Wharton, and Donald Levy for providing us with unpublished results; Anthony Merer for helpful comments on the manuscript; John Brand, John Hardwick,

and Carl Seliskar for making computer programs available to us; John Brand, Anthony Merer, and Edson Peck for making their analyses available to us prior to publication; Fred Tomkins for providing us with a Th electrodeless discharge lamp; Donald Hsu and Merrill Hessel for photographing the high resolution spectrum of $NO_2$; Charles Stevens and Rod Wallace for stimulating discussions; the Goddard Institute of Space Studies for use of their computational facilities. Support from the National Science Foundation is gratefully acknowledged.

RECEIVED: October 30, 1978

## REFERENCES

1. D. K. HSU, D. L. MONTS, AND R. N. ZARE, "Spectral Atlas of Nitrogen Dioxide: 5530 Å to 6480 Å," Academic Press, New York, 1978.
2. A. E. DOUGLAS AND K.-P. HUBER, *Canad. J. Phys.* **43,** 74–81 (1965).
3. A. E. DOUGLAS, *J. Chem. Phys.* **45,** 1007–1015 (1966).
4. K. ABÉ, *J. Mol. Spectrosc.* **48,** 395–408 (1973).
5. J. C. D. BRAND, J. L. HARDWICK, R. J. PIRKLE, AND C. J. SELISKAR, *Canad. J. Phys.* **51,** 2184–2188 (1973).
6. K. ABÉ, F. MYERS, T. K. MCCUBBIN, JR., AND S. R. POLO, *J. Mol. Spectrosc.* **38,** 552–556 (1971); **50,** 413–423 (1974); T. TANAKA, K. ABÉ, AND R. F. CURL, JR., *J. Mol. Spectrosc.* **49,** 310–313 (1974); W. DEMTRÖDER, F. PAECH, AND R. SCHMIEDL, *Chem. Phys. Lett.* **26,** 381–386 (1974); J. C. D. BRAND, J. L. HARDWICK, AND K. E. TEO, *Canad. J. Phys.* **54,** 1069–1076 (1976); H. D. BIST AND J. C. D. BRAND, *J. Mol. Spectrosc.* **62,** 60–67 (1976); J. L. HARDWICK, *J. Mol. Spectrosc.* **66,** 248–258 (1977); H. D. BIST, J. C. D. BRAND, AND A. R. HOY, *Canad. J. Phys.* **55,** 1453–1461 (1977); R. SCHMIEDL, I. R. BONILLA, AND W. DEMTRÖDER, *J. Mol. Spectrosc.* **68,** 236–252 (1977).
7. C. G. STEVENS, M. W. SWAGEL, R. WALLACE, AND R. N. ZARE, *Chem. Phys. Lett.* **18,** 465–469 (1973).
8. C. G. STEVENS AND R. N. ZARE, *J. Mol. Spectrosc.* **56,** 167–187 (1975).
9. T. TANAKA, R. W. FIELD, AND D. O. HARRIS, *J. Mol. Spectrosc.* **56,** 188–199 (1976); T. TANAKA, A. D. ENGLISH, R. W. FIELD, D. A. JENNINGS, AND D. O. HARRIS, *J. Chem. Phys.* **59,** 5217–5218 (1973); T. TANAKA, R. W. FIELD, AND D. O. HARRIS, *J. Chem. Phys.* **61,** 3401–3407 (1974); T. TANAKA AND D. O. HARRIS, *J. Mol. Spectrosc.* **59,** 413–420 (1976).
10. J. C. D. BRAND, W. H. CHAN, AND J. L. HARDWICK, *J. Mol. Spectrosc.* **56,** 309–328 (1975).
11. R. E. SMALLEY, L. WHARTON, AND D. H. LEVY, *J. Chem. Phys.* **63,** 4977–4989 (1975).
12. G. D. GILLISPIE, A. U. KHAN, A. C. WAHL, R. P. HOSTENY, AND M. KRAUSS, *J. Chem. Phys.* **63,** 3425–3444 (1975).
13. E. R. PECK, private communication (1976).
14. K. SAKURAI AND H. P. BROIDA, *J. Chem. Phys.* **50,** 2404–2410 (1969); D. NEUBERGER AND A. B. F. DUNCAN, *J. Chem. Phys.* **22,** 1693–1696 (1954); G. I. SENUM AND S. E. SCHWARTZ, *J. Mol. Spectrosc.* **64,** 75–85 (1977).
15. V. M. DONNELLY AND F. KAUFMAN, *J. Chem. Phys.* **67,** 4768–4769 (1977); 32nd Symposium on Molecular Spectroscopy, Columbus, Ohio, June 13–17, 1977, Book of Abstracts, TF5 (1977).
16. S. C. HURLOCK, K. NARAHARI RAO, L. A. WELLER, AND P. K. L. YIN, *J. Mol. Spectrosc.* **48,** 372–394 (1973).
17. G. R. BIRD, J. C. BAIRD, A. W. JACHE, J. A. HODGESON, R. F. CURL, A. C. KUNKLE, J. W. BRANSFORD, J. RASTRUP-ANDERSEN, AND J. ROSENTHAL, *J. Chem. Phys.* **40,** 3378–3390 (1964); R. M. LEES, R. F. CURL, AND J. G. BAKER, *J. Chem. Phys.* **45,** 2037–2040 (1966); P. A. BARON, P. D. GODFREY, AND D. O. HARRIS, *J. Chem. Phys.* **60,** 3723–3724 (1974).
18. C. H. TOWNES AND A. L. SCHAWLOW, "Microwave Spectroscopy," pp. 69–73, 102–105, McGraw–Hill, New York, 1955; J. T. HOUGEN, *J. Chem. Phys.* **39,** 358–365 (1963).
19. S. E. SCHWARTZ AND H. S. JOHNSTON, *J. Chem. Phys.* **51,** 1286–1302 (1969); P. B. SACKETT AND Y. T. YARDLEY, *J. Chem. Phys.* **57,** 152–167 (1972).
20. V. M. DONNELLY AND F. KAUFMAN, *J. Chem. Phys.* **66,** 4100–4110 (1977).
21. W. T. RAYNES, *J. Chem. Phys.* **41,** 3020–3032 (1964).

22. N. METROPOLIS, *Phys. Rev.* **60,** 283–294 (1941).
23. K.-E. J. HALLIN AND A. J. MERER, *Canad. J. Phys.* **55,** 2101–2112 (1977); A. J. MERER AND K.-E. J. HALLIN, *Canad. J. Phys.* **56,** 1502–1512 (1978).
24. K.-E. J. HALLIN, CH. JUNGEN, D. N. MALM, AND A. J. MERER, in preparation.
25. J. M. BROWN, J. T. HOUGEN, K.-P. HUBER, J. W. C. JOHNS, I. KOPP, H. LEFEBVRE-BRION, A. J. MERER, D. A. RAMSAY, J. ROSTAS, AND R. N. ZARE, *J. Mol. Spectrosc.* **55,** 500–503 (1975).
26. R. E. SMALLEY, L. WHARTON, AND D. H. LEVY, private communication (1976).
27. D. L. MONTS, Ph.D. Thesis, Department of Chemistry, Columbia University, New York, 1977.
28. K.-E. J. HALLIN AND A. J. MERER, *J. Mol. Spectrosc.* **65,** 163–166 (1977).
29. H. FIGGER, D. L. MONTS, AND R. N. ZARE, *J. Mol. Spectrosc.* **68,** 388–398 (1977).
30. D. L. MONTS AND R. N. ZARE, *J. Mol. Spectrosc.* **65,** 167–168 (1977).
31. A. J. MERER, private communication (1978).
32. J. C. D. BRAND, K. J. CROSS, AND A. R. HOY, *Canad. J. Phys.* **57,** 428–441 (1979).
33. A. J. MERER AND K.-E. J. HALLIN, *Canad. J. Phys.* **56,** 838–845 (1978).
34. T. C. LEE AND E. R. PECK, *J. Mol. Spectrosc.* **65,** 249–257 (1977); T. C. LEE, Ph.D. Thesis, Department of Physics, University of Idaho, Moscow, Idaho, *Diss. Abstr. Int. B* **37,** 829 (1976).
35. G. D. GILLISPIE AND A. U. KHAN, *J. Chem. Phys.* **65,** 1624–1633 (1976).